New Polynuclear Manganese(II) Complexes with Orotic Acid and some of its Derivatives: Crystal Structures, Spectroscopic and Magnetic Studies†

Francoise Nepveu,*[a] Nicolas Gaultier,*[a] Nikolaus Korber,[b] Joel Jaud[a] and Paule Castan*[a]

[a] *Université Paul Sabatier, 118 route de Narbonne, 31062-Toulouse, France*

[b] *Institut für Anorganische Chemie, Gerhard-Domagk-Str, 53121-Bonn, Germany*

Three polynuclear manganese(II) complexes containing orotic acid (2,6-dioxo-1,2,3,6-tetrahydropyrimidine-4-carboxylic acid, H_3L^1) or one of its substituted derivatives [3-methyl- (H_2L^2) or 5-nitro-2,6-dioxo-1,2,3,6-tetrahydropyrimidine-4-carboxylic acid (H_3L^1)] have been synthesized and characterized by X-ray crystallography, UV/VIS and magnetic susceptibility measurements. Complex **1** consists of neutral $[Mn_2(HL^1)_2(H_2O)_6]$ units, which form polymer chains along the *z* axis with a Mn(1) ··· Mn(2) distance in the unit cell of 5.628(1) Å while the Mn(2) ··· Mn(2) distance in the chain is 4.715(1) Å. Each unit cell of complex **2** contains one neutral centrosymmetric dimer $[Mn_2(L^2)_2(H_2O)_6]$ containing a short Mn ··· Mn distance [3.472(2) Å] and an antiferromagnetic exchange interaction is present. The experimental data were fitted to the susceptibility equations resulting from the Hamiltonian $H = -2JS_1S_2$ to give exchange parameter $J = -1.3$ cm^{-1} and $g = 1.95$. From EPR spectra of **2**, the hyperfine interaction parameter $A = -0.27$ GHz and the zero-field splitting parameter $D = \pm 2.93$ GHz have been calculated. Each unit cell of complex **3** consists of one dinuclear anion $[Mn_2(HL^3)_2(H_2O)_4Cl_2]^{2-}$ and of one cation $[K_2(H_2O)]^{2+}$. The Mn(1) and Mn(2) atoms and the water molecule of the cation $[K_2(H_2O)]^{2+}$ are situated at inversion sites. The dinuclear anions are associated to form chains but the shortest Mn ··· Mn distance of 5.642(3) Å is observed within the $[Mn_2(HL^3)_2(H_2O)_4Cl_2]^{2-}$ unit between Mn(1) and Mn(2).

Orotic acid[1] (2,6-dioxo-1,2,3,6-tetrahydropyrimidine-4-carboxylic acid, H_3L^1) is closely related to the biologically important pyrimidine bases (Fig. 1). It occupies a singular position among the free pyrimidines being the only precursor for pyrimidine bases of nucleic acids in living organisms.[1,2] The overall process of enzymatic phosphoribosylation of pyrimidinecarboxylic acids from phosphoribosylpyrophosphate ultimately requires an unsubstituted N^1 nitrogen atom.[3] In aqueous solutions, H_3L^1 acts as a diacid, with the acidic functions localized at the exocyclic carboxylic group ($pK_A = 2.09$) and at the N^3 site ($pK_A = 9.45$).[4] One of the roles played by the metal is making H_3L^1 available in the form of its reactive N^3H dianion, thus contributing to the phosphoribosylation at the N^1 site.

Its importance is also obvious as 'vitamin B_{13}' in metabolism and it is also known to display bacteriostatic and cytostatic properties.[5]

Besides its biological importance, H_3L^1 and its substituted derivatives which may be viewed as substituted pyrimidine-2,4(1*H*,3*H*)-diones are also interesting ligands since they are potentially multidentate, the co-ordination may occur through the two N atoms of the pyrimidine ring, the two carbonyl oxygens and the carboxylic group. However, studies on its co-ordination properties in solution and in the solid state show that H_3L^1 co-ordinates mainly *via* N^1 and the carboxylate group.[6–14] The only exceptions known so far are the copper(II) complex of 5-nitro-2,6-dioxo-1,2,3,6-tetrahydropyrimidine-4-carboxylic acid which co-ordinates *via* the N^1 and N^3 nitrogen[9] and the uranium complex of H_3L^1 which co-ordinates only by one oxygen of the carboxylate group.[15] Compound H_3L^1 does not enter the inner co-ordination sphere of the metal in zinc and magnesium compounds.[16,17]

† *Supplementary data available:* see Instructions for Authors, *J. Chem. Soc., Dalton Trans.*, 1995, Issue 1, pp. xxv–xxx.

Non-SI units employed: $\mu_B \approx 9.274 \times 10^{-24}$ J T^{-1}. G = 10^{-4} T.

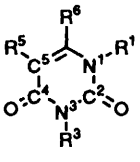

	R^1	R^3	R^5	R^6
H_3L^1	H	H	H	CO_2H
H_2L^2	H	Me	H	CO_2H
H_3L^3	H	H	NO_2	CO_2H
H_2L^4	H	H	H	CO_2Me
H_2L^5	H	H	H	H
HL^6	Me	H	H	H

Fig. 1 Numbering scheme of H_3L^3 and related compounds; H_2L^5 is pyrimidine-2,4(1*H*,3*H*)-dione and HL^6 is 1-methylpyrimidine-2,4-(1*H*,3*H*)-dione

As a part of a program oriented towards the evaluation of antioxidative properties of low-molecular weight metal complexes and accordingly with the reported superoxide radical scavenging activity of the Mn^{2+} ion in a number of *in vitro* and *in vivo* systems,[18] we studied the influence of this antioxidant effect by complexing manganese with weak ligands such as carboxylic acids.[19] Recently, we have described the quantitative analysis of such properties by EPR spectroscopy.[20] Both the biological role and the nature of these substituted carboxylic acids prompted us to investigate the radical scavenging properties of manganese(II) complexes of H_3L^1 and of some of its derivatives. Preliminary steps in this program have been to investigate the molecular structures and the physical properties of pyrimidinecarboxylate complexes with manganese.

In this paper we report on complexes of H_3L^1 and some of its derivatives *i.e.* 3-methyl- (H_2L^2), 5-nitro-2,6-dioxo-1,2,3,6-tetrahydropyrimidine-4-carboxylic acid (H_3L^3) and 2,6-dioxo-

1,2,3,6-tetrahydropyrimidine-4-methylcarboxylate (H_2L^4) with manganese(II).

Experimental

Compounds H_3L^1, H_2L^4 and the potassium salt of H_3L^3, $K_2(H_2L^3)$, were purchased from Aldrich Chemical Co. All other chemicals and solvents were reagent grade.

Synthesis of H_2L^2.—This synthesis implies the preparation of a hydantoinic ester (obtained by condensation of methylurea with an oxalacetate) and an intramolecular transposition by enlargement of the heterocycle.[21] Sodium (23 g) was slowly added to absolute ethanol (700 cm^3) and after dissolution the solvent was evaporated off. After cooling, anhydrous diethyl ether (700 cm^3) was added to the solid crust and the mixture vigorously shaken. A mixture of diethyl oxalate (146 g) and ethyl acetate (88 g) was slowly added to this suspension and stirred overnight. A sulfuric acid solution (10% in water, 300 cm^3) was then added to the yellow reaction mixture. The organic layer was decanted, neutralized by a solution of $NaHCO_3$, washed with water, and finally dried over $CaCl_2$. Distillation under reduced pressure gave $EtCO_2CH_2CO$-CO_2Et [b.p. (20 mmHg $\approx$ 2.66 $\times$ 10^3Pa) = 132 °C]. Hydrogen chloride was bubbled for 0.5 h in a mixture, maintained at 100 °C, of the oxalacetic ester (26 g), methylurea (15 g) and pure acetic acid (10 cm^3) and the reaction was kept at room temperature overnight. The crude crystalline product was washed with cold water, filtered and dried. The product so obtained, 3-methylhydantoin, was recrystallized from ethanol. This latter product (18 g) dissolved in a minimum amount of hot ethanol was refluxed for 2 h with an aqueous solution of potassium hydroxide (100 cm^3, 2 mol dm^{-3}). Ethanol was removed under reduced pressure and the residue dissolved in water. A white product was precipitated from this solution by adding diluted hydrochloric acid. Three recrystallizations gave pure H_2L^2. M.p. = 311 °C, λ_{max} = 280 nm at pH = 7.

Synthesis of $[Mn_2(HL^1)_2(H_2O)_6]$ **1**.—An aqueous solution of $MnCl_2$ (5 cm^3, 1 mmol) was added to a suspension of H_3L^1 (1 mmol) in water–ethanol (60 cm^3, 1/1) and the resulting mixture stirred for 1 h. Then the pH was adjusted to 9 by adding an ammoniacal solution (4 mol dm^{-3}) and after stirring for 2 h, the mixture was filtered off. After standing the filtrate for 3 weeks in a closed flask at room temperature, pale tan crystals were formed (Found: C, 22.45; H, 2.9; N, 10.90. Calc. for $C_5H_8MnN_2O_7$: C, 22.85; H, 3.05; N, 10.65%).

Synthesis of $[Mn_2(L^2)_2(H_2O)_6]$ **2**.—The complex was prepared by adding an aqueous solution of $MnCl_2{\cdot}4H_2O$ (1 mmol) to an aqueous solution of H_2L^2 (1 mmol) dissolved in the minimum amount of warm water (40 °C). The pH was adjusted to 7 by adding NH_4OH and then the solution was filtered off. Bright yellow crystals were formed after two weeks (Found: C, 25.9; H, 3.6; N, 10.0. Calc. for $C_6H_{10}MnN_2O_7$: C, 26.00; H, 3.65; N, 10.10%).

Synthesis of $[K_2(H_2O)][Mn_2(HL^3)_2(H_2O)_4Cl_2]$ **3**.—The salt $MnCl_2{\cdot}4H_2O$ (1.5 mmol in the minimum of water) was added to an aqueous solution of the potassium salt of H_3L^3 (15 cm^3, 1 mmol). The solution was kept at 40 °C, with stirring during 2 h. At this time the pH of the reaction mixture was 2. The pH was then increased to 7.6 by slowly adding a water–triethylamine solution (4:1). After stirring vigorously for 5 h, the solution was filtered off and diluted with acetonitrile (8 equivalents). By leaving the resulting deep yellow solution in a closed flask containing glass fibres, yellow crystals were collected on the fibres within 5 d and were washed with diethyl ether (Found: C, 15.65; H, 1.45, Cl, 9.60; Mn, 14.25; N, 10.90. Calc. for $C_5H_6ClKMnN_3O_{8.5}$: C, 16.05; H, 1.60; Cl, 9.49; Mn, 14.70; N, 11.25%).

Attempted Synthesis of the Complex of the Methyl ester of H_3L^1.—An equivalent amount of H_2L^4 in a minimum amount of hot water was added to a solution of $MnCl_2{\cdot}4H_2O$. On standing at room temperature the solution rapidly yielded pale yellow crystals (Found: C, 22.9; H, 3.05; N, 10.8%).

Physical Measurements.—Elemental analyses were carried out at Service Interuniversitaire de Microanalyse, Toulouse; UV spectra were recorded on a SECOMAM S 1000 spectrometer in aqueous solutions; IR spectra were recorded on a Perkin-Elmer 983 G spectrometer coupled with a Perkin-Elmer infrared data station with samples run in the solid state (KBr pellets). Variable-temperature magnetic susceptibility data were collected on powdered samples of the compounds with use of a SQUID-based sample magnetometer on a Quantum Design Model MPMS instrument. All data were corrected for diamagnetism of the ligands estimated from Pascal's constants.[22] The EPR spectra were recorded on a Bruker ESP 300E spectrometer and were run either in the solid state (300 and 120 K) or as water or water–ethylene glycol (ethane-1,2-diol) glasses at 100 K.

X-Ray Crystal Structure Determinations.—Graphite-monochromated Mo-Kα radiation (λ = 0.710 73 Å) was employed as X-ray source for all studies. X-Ray diffraction measurements were made using an ENRAF NONIUS CAD4 diffractometer for **1** and a Stoe-Stadi-4 diffractometer for **2** and **3**. Intensity data were collected at 295 K with ω–2θ scan mode. Crystal data, intensity measurements and structure refinements are summarized in Table 1. The data were corrected for Lorentz, polarization and absorption effects with empirical absorption correction. Transmission factors are given in Table 1. The structures were solved using direct methods and final refinements involve absorption corrected data and anisotropic refinement for all non-hydrogen atoms. Residuals R and R' are given in Table 1. For complex **3**, the quantity minimized was wR_2 using all reflections with $wR_2 = [(\Sigma\{w(F_o^2 - F_c^2)^2/\Sigma(w(F_o^2)^2\}]^{\frac{1}{2}}$ (= 0.0877). The R and R' values are also given in Table 1 for comparison with complexes **1** and **2**. Program packages used for calculations, refinements and plotting were successively, SHELXS 86,[23] CRYSTALS[24] and PLATON-90[25] for **1**, SHELXS 86,[23] ORFFE-3[26] and SHELXTL PLUS[27] for **2** and SHELXS 86[23] and SHELXL 93[28] for **3**. The program KPLOT[29] was used for plotting the structure of the compouunds. Atomic scattering factors and anomalous dispersion terms were obtained from program packages or from ref. 30. All hydrogen atoms have been observed on Fourier-difference maps and refined with fixed isotropic thermal parameters for **1**, and free isotropic thermal parameters for **2** and **3**. Non-hydrogen atom positional parameters with estimated standard deviations (e.s.d.s) are gathered in Tables 2–4 for complexes **1**–**3**, respectively. Selected interatomic distances and angles are listed in Tables 2–5 and plots of the molecules are shown in Figs. 2–6 along with the labelling schemes.

Additional material available from the Cambridge Crystallographic Data Centre comprises H-atom coordinates, thermal parameters and remaining bond lengths and angles.

Results and Discussion

Synthesis.—It was shown potentiometrically that when the esters of H_3L^1 are used as metal complexing agents no complexation was observed. This indicates the important role played by N^1 and the carboxylate group for metal chelation. Although a complex has been obtained by treating H_2L^4 with a manganese(II) salt, the results of chemical analysis were not in accord with a complex of H_2L^4 but rather with H_3L^1 itself. This suggests that during the reaction process, hydrolysis of the ester function occurs. We have already observed hydrolysis of the ester function for a palladium complex and a crystal structure

Table 1 Summary of crystal data, intensity measurements and structure refinement

Compound	1	2	3
Empirical formula	$C_{10}H_{16}Mn_2N_4O_{14}$	$C_{12}H_{20}Mn_2N_4O_{14}$	$C_5H_6ClKMnN_3O_{8.5}$
M	526.1	554.2	373.6
Crystal system	Monoclinic	Triclinic	Triclinic
Space group	$P2_1/n$	$P\bar{1}$	$P\bar{1}$
a/Å	7.367(2)	6.575(1)	7.291(1)
b/Å	28.569(5)	8.577(1)	9.014(2)
c/Å	8.449(3)	9.608(2)	10.002(2)
α/°		64.54(1)	70.45(1)
β/°	96.24(7)	83.01(1)	79.80(1)
γ/°		89.97(1)	68.45(1)
U/Å^3	1767.8	484.8	575.0
Z	4	1	2
D_c/g cm^{-3}	1.98	1.89	2.16
$F(000)$	1064	282	372
μ(Mo-Kα)/cm^{-1}	14.5	13.0	17.9
hkl	0–10, 0–40, −11 to 11	−20 to 20, −11 to 11, 0–18	−9 to 9, −10 to 11, −12 to 12
Scan range 2θ/°	2–60	5–60	4.32–55
Transmission factors (min., max.)	0.84, 1.00	0.775, 0.874	0.71, 0.89
No. of measured reflections	4819	3515	3236
No. of independent reflections	4199	2719	2622
No. of observed reflections	4188	2548	2304
No. of parameters	272	186	208
Criterion for observed reflections	$I \geqslant 3\sigma(I)$	$F_o \geqslant 3\sigma(F_o)$	$F_o \geqslant 4\sigma(F_o)$
Refinement	F	F	F^2
R, R'	0.031, 0.039	0.037, 0.033	0.0323, 0.0827
Max., min. $\Delta\rho$/e Å^{-3}	0.15, −0.4	0.82, −0.58	0.435, −1.254

Table 2 Positional parameters for non-hydrogen atoms of complex **1** with e.s.d.s in parentheses

Atom	x	y	z
Mn(1)	0.119 95(5)	0.277 56(1)	−0.136 00(4)
Mn(2)	0.192 55(5)	0.087 68(1)	0.036 64(4)
O(1)	0.041 6(3)	0.276 08(6)	0.105 2(2)
O(2)	0.255 0(3)	0.385 43(6)	−0.259 9(2)
O(3)	0.020 6(3)	0.315 21(6)	0.328 4(2)
O(4)	0.210 9(4)	0.478 82(7)	0.164 8(3)
O(5)	0.387 9(3)	0.256 96(8)	−0.026 1(2)
O(6)	−0.161 0(3)	0.296 32(7)	−0.230 7(2)
O(7)	0.257 2(3)	0.288 70(7)	−0.351 0(2)
O(8)	0.056 7(3)	0.208 80(6)	−0.236 7(2)
O(9)	0.084 7(3)	0.156 62(6)	−0.039 3(2)
O(10)	0.204 2(3)	0.009 81(7)	−0.279 3(2)
O(11)	0.224 2(3)	0.108 39(7)	0.301 2(2)
O(12)	0.454 9(3)	0.118 58(9)	0.033 3(2)
O(13)	0.335 5(3)	0.020 58(7)	0.064 3(2)
O(14)	−0.057 2(3)	0.054 62(7)	0.083 1(3)
N(1)	0.160 4(3)	0.350 55(7)	−0.041 4(2)
N(2)	0.228 8(3)	0.430 49(7)	−0.044 0(2)
N(3)	0.152 5(3)	0.086 88(7)	−0.232 8(2)
N(4)	0.205 1(3)	0.059 73(7)	−0.487 4(2)
C(1)	0.215 6(3)	0.387 94(8)	−0.118 4(3)
C(2)	0.195 2(4)	0.438 20(9)	0.110 3(3)
C(3)	0.142 5(4)	0.397 92(9)	0.192 7(3)
C(4)	0.124 5(3)	0.356 55(8)	0.111 9(3)
C(5)	0.057 5(3)	0.312 56(8)	0.189 1(3)
C(6)	0.186 9(4)	0.051 02(8)	−0.328 3(3)
C(7)	0.193 1(3)	0.103 33(8)	−0.556 4(3)
C(8)	0.147 1(3)	0.140 03(8)	−0.454 7(3)
C(9)	0.129 5(3)	0.129 82(8)	−0.299 1(3)
C(10)	0.085 7(3)	0.168 07(8)	−0.181 5(3)

Table 3 Positional parameters for non-hydrogen atoms of complex **2** with e.s.d.s in parentheses

Atom	x	y	z
Mn	0.4173(1)	0.3006(1)	0.1520(1)
O(1)	0.7336(3)	0.2678(3)	0.2302(2)
O(2)	0.1328(3)	0.3111(3)	0.0538(3)
O(3)	0.3788(3)	0.0262(2)	0.2714(2)
N(1)	0.2957(3)	0.3355(2)	0.3645(2)
C(1)	0.2392(3)	0.2072(3)	0.5091(3)
O(4)	0.2271(3)	0.0523(2)	0.5333(2)
N(2)	0.1952(3)	0.2484(2)	0.6346(2)
C(2)	0.1335(5)	0.1076(3)	0.7910(3)
C(3)	0.2044(3)	0.4162(3)	0.6188(3)
O(5)	0.1677(3)	0.4454(2)	0.7366(2)
C(4)	0.2594(3)	0.5472(3)	0.4654(3)
C(5)	0.3024(3)	0.5015(3)	0.3469(3)
C(6)	0.3714(3)	0.6390(3)	0.1828(3)
O(6)	0.3663(3)	0.7930(2)	0.1531(2)
O(7)	0.4314(3)	0.5805(2)	0.0835(2)

has evidenced that H_2L^4 was demethylated during the co-ordination process.[31] The comparatively slow rate of hydrolysis of H_2L^4 is thus increased in the presence of a metal.

Solution Study.—Relationships between complexation sites of pyrimidine derivatives and UV data have been reported. From the UV data characterizing the N^1 and/or N^3 methylated 2,6-dioxo-1,2,3,6-tetrahydropyrimidine-4-carboxylic acids,[32–34] pyrimidine-2,4(1*H*,3*H*)-diones,[35,36] and their related anions, one can predict the sites of deprotonation and co-ordination.

In the previously reported nickel(II)[6] and copper(II)[7] complexes, the observed bathochromic shift from the free ligand to the complex may be related to the predominance of the N^3H form and to the concomitant co-ordination of the metal to N^1, also established by X-ray structural determinations. The relationship between the UV data and the co-ordination sites is further supported by the marked change of UV spectra of H_2L^2 upon complexation by nickel(II) which unambiguously occurs at N^1.[37] These results show that absorbance of a complex >310 nm indicates complexation by N^1 and thus infers the existence of a N^3H tautomer (or of a substituted N^3), while absorbance in the range 280–290 nm infers complexation at N^3. As already mentioned only one complex, the copper(II) complex of H_3L^3, has so far been obtained which displays complexation by both N^1 and N^3; potentiometric titrations also show that the copper(II) ion removes all the replaceable protons.

Table 4 Positional parameters for non-hydrogen atoms of complex **3** with e.s.d.s in parentheses

Atom	*x*	*y*	*z*
Mn(1)	0	0	1.0000
K(1)	0.1612(1)	0.7948(1)	0.3920(1)
O(1)	0.2716(3)	−0.0422(2)	1.0985(2)
N(1)	0.1173(3)	−0.2638(2)	1.0000(2)
C(1)	0.0927(3)	−0.3910(3)	1.1148(2)
O(2)	−0.0071(3)	−0.3651(2)	1.2222(2)
N(2)	0.1871(3)	−0.5528(2)	1.1073(2)
C(2)	0.3004(3)	−0.5982(3)	0.9932(2)
O(3)	0.3802(3)	−0.7467(2)	0.9990(2)
C(3)	0.3092(3)	−0.4571(3)	0.8735(2)
N(3)	0.4094(3)	−0.4947(2)	0.7441(2)
O(4)	0.5825(3)	−0.5846(3)	0.7501(2)
O(5)	0.3166(3)	−0.4437(3)	0.6387(2)
C(4)	0.2239(3)	−0.2975(2)	0.8835(2)
C(5)	0.2572(3)	−0.1445(3)	0.7702(2)
O(7)	0.3790(3)	−0.1696(2)	0.6694(2)
O(6)	0.1635(3)	−0.0062(2)	0.7918(2)
Mn(2)	0.5000	0	0.5000
Cl(1)	0.1774(1)	0.1356(1)	0.3786(1)
O(8)	0.4026(3)	0.1907(3)	0.6154(3)
O(9)	0.0869(9)	0.4657(7)	0.4935(5)

In an attempt to elucidate the metal–ligand binding mode of Mn^{II} towards H_3L^1 or its derivatives in solution, UV absorption spectra of the free ligands, of ligand–Mn^{II} salt mixtures in different ratios and of the isolated complexes (**1**–**3**) were recorded and compared.

For the isolated complex **1**, no bathochromic shift in the maximum absorbance wavelength (λ_{max} = 284 nm) with respect to the free dianion, HL^1, (λ_{max} = 285–290 nm) was observed in aqueous solution. This was not the case with copper and nickel complexes of H_3L^1 [37] for which complexation induced a significant bathochromic shift of the ligand absorption band (λ_{max} = 316 nm). When the UV studies were performed on ligand–Mn^{II} salt mixtures, a bathochromic shift in the spectrum (λ_{max} = 304 nm) was observed at high ligand : metal ratio (1 : 20) suggesting a classical co-ordination of the metal to N^1 and to the carboxylate group. These results indicate that complex **1** dissociates in aqueous solution and has a low stability since complexation is only observed in the presence of a large excess of metal salt. This agrees with potentiometric studies which have shown that H_3L^1 forms only very weak complexes with manganese.[4]

For the isolated complex **2**, a significant bathochromic shift in the maximum absorption band (λ_{max} *ca.* 300 nm) with respect to the free acid (H_2L^2, λ_{max} = 278 nm) is observed. This shift is comparable with those observed for the nickel, copper and palladium complexes [37,38] implying a complexation at the N^1 and carboxylate chelating sites. By contrast, adding manganese(II) salt to a solution of H_2L^2 does not induce a significant bathochromic shift even with a large metal salt excess (1 : 40). These results indicate that Mn^{II} is only weakly complexed by H_2L^2 in solution, in contrast to Cu^{II} and Ni^{II} ions which form more stable complexes with that acid than with H_3L^1 itself.[37] However, once isolated by slow evaporation, **2** does not dissociate, or if so, only partially in aqueous solution as indicated by the observable bathochromic shift. This stability in solution agrees well with the dinuclear structure of complex **2** in the solid state for which a short metal–metal distance is observed (see below).

Linear free energy relationships for proton dissociation and metal complexation have been observed for the pyrimidine acid system.[32] Considering the acid dissociation constants of H_3L^3 (pK_1 and pK_2 of 1.5 and 4.94, respectively) relative to those of H_3L^1 (2.07 and 9.45), one might expect the metal complexes of H_3L^3 to be more stable than the corresponding H_3L^1 complexes. Introduction of a nitro group, which was found to have a pronounced effect on the dissociation constants determined potentiometrically, also induces considerable modification of the UV spectra. Thus, at the same acidic pH, H_3L^1 exhibits a band at 285 nm while H_3L^3 shows a band at 297 nm. In basic or neutral media the same band was found to shift to 338 nm implying a N^1 deprotonation for H_3L^3. In solution, complex **3** exhibits a band at 340 nm and when the UV measurement was performed on aqueous ligand–metal salt mixtures, the same absorption was observed whatever the ligand : metal ratio. These results are in agreement with a binding mode at the N^1 CO_2-chelating site and suggest a stronger complexing effect of H_3L^3 compared to H_3L^1 and H_2L^2 toward Mn^{II}.

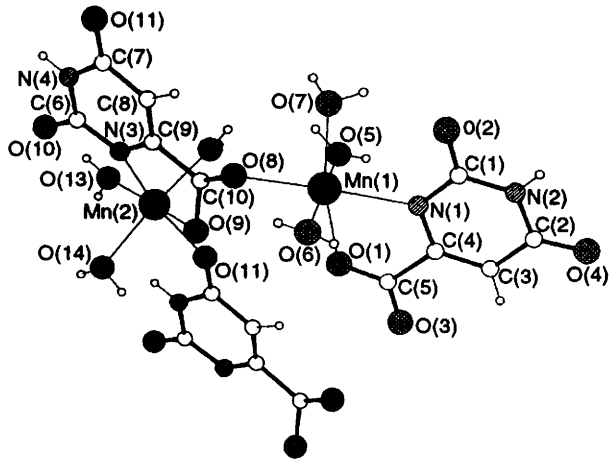

Fig. 2 Structure of compound **1**

Description of the Structure of Complex **1**.—The complex contains two different types of manganese atom and also two different HL^1 anions. Complex **1** consists of neutral $[Mn_2(HL^1)_2(H_2O)_6]$ units which are bonded to each other to form polymer chains along the *z* axis. The core of the chain consists of Mn(2) and the HL^1 anion 2 and the co-ordination sphere at the manganese atoms is shown in Fig. 2. Each manganese atom is bonded to one HL^1 anion at ring nitrogen N^1 and at the adjacent carboxylate oxygen. For Mn(1) the six-co-ordination (NO_2O_{w3}) is completed by the oxygen of the carboxylate group of other HL^1 anion bonded to Mn(2) and thus the HL^1 anion 1 is bidentate (N^1, O^1). The remainder of the co-ordination sites around Mn(1) are occupied by three water molecules. For Mn(2) the six-co-ordination (NO_2O_{w3}) is completed by an exocyclic keto oxygen (O^{11}) of the HL^1 anion 2 of another unit and thus the HL^1 anion 2 is tetradentate (O^8, O^9, O^{11}, N^3) and bridges two Mn(2) metal ions by an *anti-syn* type of carboxylate bridge forming polymer chains of dinuclear units along the *z* axis (Fig. 3). The remainder of the co-ordination sites at Mn(2) are occupied by three water molecules. The Mn(1)···Mn(2) distance in the unit cell is 5.628(1) Å while the Mn(2)···Mn(2) distance in the chain is 4.715(1) Å (Table 5). In a copper(II) HL^1 complex[9] the two C–O bond lengths at the carboxylate group are quite different, 1.267(4) and 1.225(4) Å, with that bonded to Cu being the longer. This is observed in many complexes of HL^1. By contrast, in the manganese complex **1** the two C–O bond lengths of the carboxylate group of the HL^1 anion 2 are nearly the same [C(10)–O(8) 1.263(3), C(10)–O(9) 1.246(3) Å] respectively. Similarly the Mn(1)–O(1) and Mn(1)–O(8) distances at 2.178(2) and 2.171(2) Å, respectively are almost identical. The co-ordination at the HL^1 anion 1 is typical of that of classical complexes with two different carboxylate C–O bonds, with one of the oxygens co-ordinated to Mn(1) having a long C–O bond

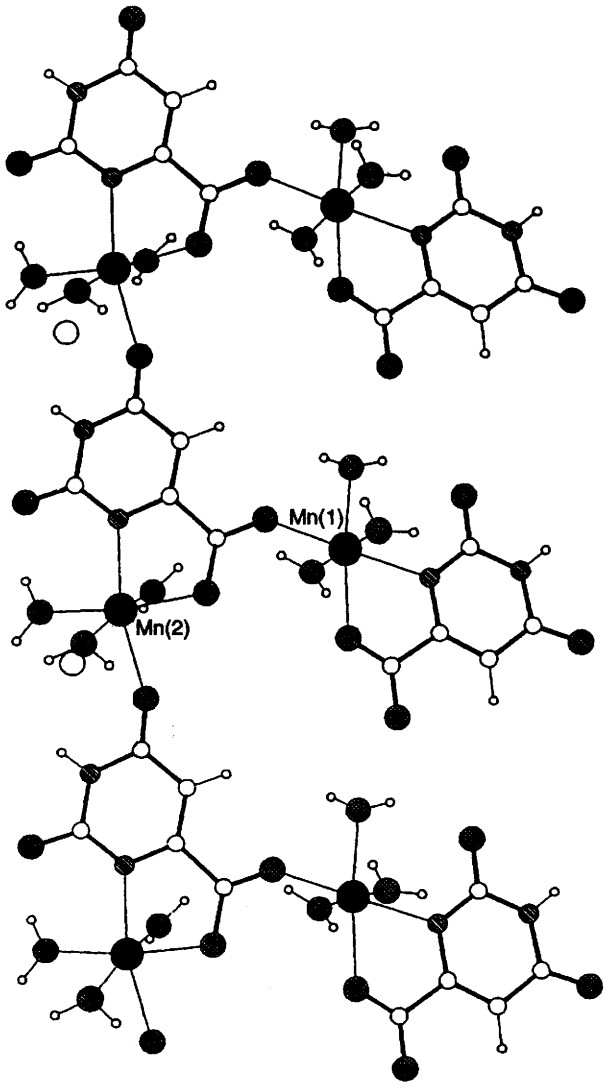

Fig. 3 Representation of the polymeric structure of compound 1

distance of 1.259(3) Å and the oxygen not co-ordinated having a short C–O bond distance of 1.239(3) Å. The Mn–O distances are fairly similar except for Mn(2)–O(11), 2.299(2) Å, between the Mn(2) atom and the exocyclic oxygen of the pyrimidine ring, this distance is also longer than that observed in polymeric nickel or cobalt HL^1 complexes where all M–O distances are similar at *ca.* 2.10 Å whatever the type of oxygen involved (carboxylate, water or exocyclic keto oxygen).[10] Structural parameters for the HL^1 anion compared to those of monohydrated H_3L^1[39] show rather similar bond lengths while the bond angles display some marked differences. It should be noted that the carbonyl bond lengths are quite similar whether the carbonyl group is co-ordinated or not and co-ordination to the metal does not influence the CO bond order. The C(4)–N(1)–C(1) [117.6(2)°] and C(9)–N(3)–C(6) [117.8(2)°] angles are clearly smaller than in H_3L^1 (122.7°)[39] due to the complexation of the metal by the corresponding nitrogen atoms. Correlatively the C(3)–C(4)–N(1) and the C(8)–C(9)–N(3) angles [124.5(2)° and 124.9(2)°, respectively] are increased relative to that of H_3L^1 (121.7°).

The pyrimidine ring deviates only very slightly from planarity. The dihedral angle between pyrimidine ring 1 and the co-ordination ring plane of Mn(1) is 2.29°, while that between pyrimidine ring 2 and the co-ordination ring plane of Mn(2) is 10.08°

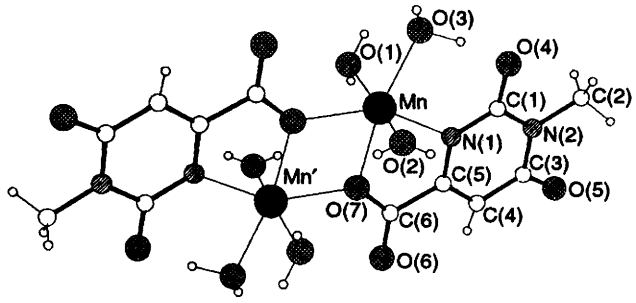

Fig. 4 Structure of the dinuclear compound 2

Table 5 Selected interatomic distances (Å) and bond angles (°) with e.s.d.s in parentheses for complex 1

Mn(1)–O(1)	2.178(2)	Mn(2)–O(9)	2.193(2)
Mn(1)–O(5)	2.169(2)	Mn(2)–O(11)	2.299(2)
Mn(1)–O(6)	2.202(2)	Mn(2)–O(12)	2.128(2)
Mn(1)–O(7)	2.196(2)	Mn(2)–O(13)	2.188(2)
Mn(1)–O(8)	2.171(2)	Mn(2)–O(14)	2.142(2)
Mn(1)–N(1)	2.242(2)	Mn(2)–N(3)	2.264(2)
Mn(1)···Mn(2)	5.628(1)	Mn(2)···Mn(2)	4.715(1)
O(1)–Mn(1)–N(1)	73.90(7)	O(9)–Mn(2)–N(3)	73.22(7)
N(1)–Mn(1)–O(7)	96.02(7)	N(3)–Mn(2)–O(13)	96.15(7)
O(7)–Mn(1)–O(8)	84.58(7)	O(13)–Mn(2)–O(11)	97.17(7)
O(8)–Mn(1)–O(1)	106.36(7)	O(11)–Mn(2)–O(9)	92.79(7)
O(5)–Mn(1)–N(1)	91.16(8)	O(12)–Mn(2)–N(3)	90.58(8)
O(5)–Mn(1)–O(7)	85.06(8)	O(12)–Mn(2)–O(13)	86.42(9)
O(5)–Mn(1)–O(8)	93.95(8)	O(12)–Mn(2)–O(11)	84.82(8)
N(1)–Mn(1)–O(8)	174.89(7)	N(3)–Mn(2)–O(11)	165.60(7)
Ligand 1		Ligand 2	
C(4)–N(1)	1.361(3)	C(9)–N(3)	1.352(3)
C(1)–N(1)	1.337(3)	C(6)–N(3)	1.345(3)
C(1)–N(2)	1.367(3)	C(6)–N(4)	1.388(3)
C(2)–N(2)	1.370(3)	C(7)–N(4)	1.374(3)
C(2)–C(3)	1.421(3)	C(7)–C(8)	1.420(3)
C(3)–C(4)	1.364(3)	C(8)–C(9)	1.367(3)
C(4)–C(5)	1.522(3)	C(9)–C(10)	1.534(3)
C(5)–O(1)	1.259(3)	C(10)–O(9)	1.246(3)
C(5)–O(3)	1.239(3)	C(10)–O(8)	1.263(3)
C(1)–O(2)	1.263(3)	C(6)–O(10)	1.250(3)
C(2)–O(4)	1.249(3)	C(7)–O(11)	1.258(3)
C(4)–N(1)–C(1)	117.6(2)	C(9)–N(3)–C(6)	117.8(2)
N(1)–C(1)–N(2)	119.8(2)	N(3)–C(6)–N(4)	119.3(2)
N(2)–C(2)–C(3)	115.0(2)	N(4)–C(7)–C(8)	114.9(2)
C(2)–C(3)–C(4)	118.2(2)	C(7)–C(8)–C(9)	118.6(2)
C(3)–C(4)–N(1)	124.5(2)	C(8)–C(9)–N(3)	124.9(2)
O(1)–C(5)–O(3)	124.7(2)	O(8)–C(10)–O(9)	125.4(2)
N(1)–C(4)–C(5)	114.2(2)	N(3)–C(9)–C(10)	113.8(2)

The polymeric chains are held together by an extensive array of hydrogen bonds details of which are given in Table 6.

Description of the Structure of Complex **2**.—Each unit cell of $[Mn_2(L^2)_2(H_2O)_6]$ contains one discrete neutral centrosymmetric dimer (Fig. 4). The two manganese atoms Mn and Mn' are bridged by oxygens O(7) and O(7') from two carboxylate groups. Each metal is six-co-ordinate (NO_2O_{w3}) with further co-ordination to the deprotonated N^1 nitrogen atoms of the pyrimidine ring adjacent to the carboxylate group, and to three water molecules. Carboxylate bridging between transition-metal atoms is well known in complexes such as copper(II) acetate hydrate.[40,41] This mode of bridging links adjacent metal atoms *via* two different oxygens of a carboxylate group to form M–O–C–O–M bridges (*syn-syn*, *anti-anti* or *anti-syn*). However, it is an obvious *a priori* possibility that carboxylate

Table 6 Distances (Å) and angles (°) of hydrogen bonds D–H · · · A, for complex **1**; D = donor atom, A = acceptor atom

D	H	A	D · · · A	D–H	H · · · A	D–H · · · A
N(2)	H(21)	O(10^{IV})	2.787(3)	0.84	1.95	177
N(4)	H(41)	O(4^{V})	2.859(3)	0.86	2.00	174
O(5)	H(51)	O(8^{I})	2.797(3)	0.84	1.98	163
O(5)	H(52)	O(3^{IV})	2.642(3)	0.93	1.73	164
O(6)	H(61)	O(11^{II})	2.872(3)	0.83	2.06	171
O(6)	H(62)	O(1^{III})	3.216(4)	0.89	2.50	138
O(6)	H(62)	O(5^{III})	2.979(3)	0.89	2.50	134
O(7)	H(71)	O(1^{IV})	2.850(3)	0.90	1.95	176
O(7)	H(72)	O(2^{I})	2.869(3)	0.88	2.16	138
O(12)	H(121)	O(2^{I})	2.667(3)	0.86	1.83	165
O(12)	H(122)	O(3^{I})	2.645(3)	0.90	1.75	178
O(13)	H(131)	O(10^{I})	2.974(3)	0.86	2.21	150
O(13)	H(132)	O(4^{VI})	2.636(3)	0.90	1.77	161
O(14)	H(141)	O(2^{II})	2.647(3)	0.85	1.80	176
O(14)	H(142)	O(10^{I})	2.775(3)	0.90	2.07	135

Symmetry operations: I x, y, z; II $-\frac{1}{2}+x, \frac{1}{2}-y, \frac{1}{2}+z$; III $-\frac{1}{2}+x, \frac{1}{2}-y, -\frac{1}{2}+z$; IV $\frac{1}{2}+x, \frac{1}{2}-y, -\frac{1}{2}+z$; V $\frac{1}{2}+x, -\frac{1}{2}-y, -\frac{1}{2}+z$; VI $\frac{1}{2}+x, -\frac{1}{2}-y, \frac{1}{2}+z$.

Table 7 Selected interatomic distances (Å) and bond angles (°) with e.s.d.s in parentheses for complex **2**

Mn–O(1)	2.273(2)	Mn–O(2)	2.180(8)
Mn–O(3)	2.128(2)	Mn–N(1)	2.241(2)
Mn–O(7)	2.199(2)	Mn–O(7′)	2.149(4)
Mn · · · Mn′	3.472(2)		
O(1)–Mn–O(3)	85.7(1)	O(2)–Mn–O(3)	90.6(1)
O(1)–Mn–N(1)	89.1(1)	O(2)–Mn–N(1)	99.6(1)
O(1)–Mn–O(7)	93.2(1)	O(2)–Mn–O(7)	92.4(1)
N(1)–Mn–O(7)	73.4(1)	Mn–O(7)–Mn′	106.0(1)
C(1)–N(1)	1.357(3)	C(1)–N(2)	1.394(3)
C(1)–O(4)	1.247(3)	C(2)–N(2)	1.474(3)
C(3)–N(2)	1.382(3)	C(3)–O(5)	1.256(2)
C(3)–C(4)	1.418(3)	C(4)–C(5)	1.355(3)
C(5)–C(6)	1.520(3)	C(5)–N(1)	1.360(3)
C(6)–O(6)	1.227(3)	C(6)–O(7)	1.280(2)
N(1)–C(1)–O(4)	121.6(2)	N(1)–C(1)–N(2)	119.5(2)
C(1)–N(1)–C(5)	118.2(2)	O(4)–C(1)–N(2)	118.9(2)
C(1)–N(2)–C(2)	118.9(2)	C(1)–N(2)–C(3)	122.9(2)
C(2)–N(2)–C(3)	118.2(2)	O(5)–C(3)–N(2)	120.1(2)
N(2)–C(3)–C(4)	116.1(2)	O(5)–C(3)–N(4)	123.9(2)
C(3)–C(4)–C(5)	119.2(2)	C(4)–C(5)–N(1)	124.1(2)
N(1)–C(5)–C(6)	115.7(2)	C(4)–C(5)–C(6)	120.1(2)
O(6)–C(6)–C(5)	120.4(2)	O(6)–C(6)–O(7)	124.7(2)

can be involved in a monoatomic bridging mode forming an M–O–M bridge. The occurrence of such bridges is however firmly established in only a few cases.[42–44] While in complex **1** the carboxylate group acts as a bridge between two metal atoms using both oxygen atoms, in complex **2** the same oxygen of the carboxylate group is three-co-ordinate and bridges two metal atoms. This unusual bonding mode results in a significant difference between the two C–O bond lengths, 1.280(2) Å and 1.227(3) Å, for the bridging and free carboxylate oxygens respectively. Consequently, the Mn · · · Mn distance is short [3.472(2) Å] and the Mn–O(7)–Mn′ angle is 106.0(1)° (Table 7). The geometry at the metal is quite distorted from octahedral because of the steric hindrance arising from the small bite angle N(1)–Mn–O(7) of 73.4(1)°. As expected, the bond lengths at the pyrimidine ring are normal and do not differ from those of H_3L^1 itself.

Description of the Structure of Complex **3**.—Each unit cell of complex **3** consists of one dinuclear anion $[Mn_2(HL^3)_2(H_2O)_4Cl_2]^{2-}$ and of one $[K_2(H_2O)]^{2+}$ cation. The dinuclear anions are bonded together to form infinite chains. The co-

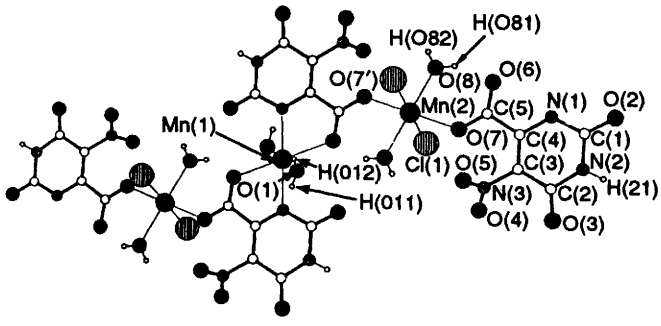

Fig. 5 Structure of the dinuclear anion $[Mn_2(HL^3)_2(H_2O)_4Cl_2]^{2-}$ of compound **3**

ordination spheres about the two manganese atoms Mn(1) and Mn(2) are shown in Fig. 5 and interatomic distances and angles are given in Table 8. The Mn(1) manganese atom situated at an inversion centre is six-co-ordinated ($N_2O_2O_{W2}$) by two HL^3 anions at ring nitrogen N(1) and N(1′), at adjacent carboxylate oxygens O(6) and O(6′) and by two water molecules O(1) and O(1′). All the bond lengths around Mn(1) are quite similar but the angles differ significantly from the ideal value of 90° because of the steric hindrance arising from the small co-ordination bite angle [N(1)–Mn(1)–O(6) 72.98(6)°]. Complex **3** is the second example where two pyrimidinecarboxylate ligands are bonded by N(1) and by the carboxylate oxygen to the same metal atom, the previously described example being the cadmium complex of H_3L^1.[13] However, these two complexes are not isostructural. The Mn(2) atom is also situated at an inversion centre, the six-co-ordination ($Cl_2O_2O_{W2}$) being provided by two chlorine atoms Cl(1) and Cl(1′), two water molecules O(8) and O(8′) and by the other oxygens O(7) and O(7′) of the carboxylate groups of the HL^3 anions bonded to Mn(1). Thus the HL^3 anions are tridentate, with the carboxylate group acting as an *anti-syn* bridge between the two metal atoms Mn(1) and Mn(2), as shown in Fig. 5. The manganese–ligand lengths are quite different around Mn(2) due to the manganese–chlorine co-ordination. However, the angles are little distorted from the ideal values. The Mn–O bond distances around Mn(1) and Mn(2) are quite similar and the negative charge of the carboxylate group is equally distributed between the two metal atoms.

The shortest Mn · · · Mn distance in the $[Mn_2(HL^3)_2(H_2O)_4Cl_2]^{2-}$ unit is between Mn(1) and Mn(2) with a value of 5.642(3) Å.

The water molecule O(9) is situated at an inversion centre and bridges the two potassium atoms K(1) and K(1′). Atom O(9) is

Table 8 Selected interatomic distances (Å) and bond angles (°) with e.s.d.s in parentheses for complex **3**

Mn(1)–O(1)	2.219(2)	Mn(2)–O(7)	2.171(2)
Mn(1)–N(1)	2.211(2)	Mn(2)–Cl(1)	2.531(8)
Mn(1)–O(6)	2.216(2)	Mn(2)–O(8)	2.221(2)
Mn(1)···Mn(2)	5.642(3)		
O(1)–Mn(1)–N(1)	88.66(7)	O(7)–Mn(2)–Cl(1)	91.32(6)
O(1)–Mn(1)–O(6)	91.79(7)	O(7)–Mn(2)–O(8)	92.54(8)
N(1)–Mn(1)–O(6)	72.98(6)	Cl(1)–Mn(2)–O(8)	89.89(7)
C(1)–N(1)	1.365(3)	C(1)–N(2)	1.387(3)
C(2)–N(2)	1.372(3)	C(2)–C(3)	1.438(3)
C(3)–C(4)	1.373(3)	C(4)–C(5)	1.532(3)
C(4)–N(1)	1.341(3)	C(5)–O(6)	1.253(3)
C(5)–O(7)	1.243(3)	C(1)–O(2)	1.227(3)
C(2)–O(3)	1.234(3)	C(3)–N(3)	1.450(3)
N(3)–O(4)	1.223(3)	N(3)–O(5)	1.216(3)
C(4)–N(1)–C(1)	119.8(2)	N(1)–C(1)–N(2)	117.7(2)
N(2)–C(2)–C(3)	112.8(2)	C(2)–C(3)–C(4)	120.8(2)
C(3)–C(4)–N(1)	122.4(2)	O(6)–C(5)–O(7)	126.4(2)
N(1)–C(4)–C(5)	113.8(2)	O(4)–N(3)–O(5)	123.6(2)
K(1)···Cl(1^{IV})	3.074(2)	K(1)···O(1^{III})	2.927(2)
K(1)···O(9)	3.016(6)	K(1)···O(6^{II})	2.915(2)
K(1)···O(4^{I})	2.714(2)	K(1)···Cl(1^{II})	3.094(2)
K(1)···O(5^{I})	2.765(2)		

Symmetry transformations used to generate equivalent atoms: I $-x+1, -y, -z+1$; II $-x, -y+1, -z+1$; III $x, y+1, z-1$; IV $x, y+1, z$.

disordered over two sites, but is well behaved and the atomic displacement parameters are normal (see supplementary data). Other ionic interactions between the potassium ion and the chlorine atoms, the oxygen O(5) of the nitro group, and some of the water molecules bonded to manganese are also observed (Table 8, Fig. 6).

In this structure, as in all the structures which contain HL^1, whether complexed or not, the respective bond lengths in the pyrimidine ring are quite similar, showing that complexation does not affect the π delocalization.

Magnetic Susceptibility.—The magnetic susceptibilities for complexes **1**–**3** were measured in the range 290–2 K. At room temperature, complexes **1**, **2** and **3** have effective magnetic moments per manganese(II) ion of 5.83, 5.66 and 5.86 μ_B, respectively, indicating the high-spin nature of each complex.

The effective magnetic moment per manganese(II) decreases slowly from 5.83 to 5.50 μ_B and from 5.86 to 5.41 at 8 K for complexes **1** and **3**, respectively. Below 8 K the magnetic moment decreases more dramatically and reaches 4.40 and 4.24 μ_B per Mn at 2 K for complexes **1** and **3**, respectively. The results of the crystal structure determination of complex **1** indicates a chain structure of dinuclear units with a Mn(2)···Mn(2) distance of 4.715(1) Å within the chain and a Mn(1)···Mn(2) distance of 5.628(1) Å in the dinuclear unit. Moreover no Mn···Mn interchain distances below 4.715 Å are observed. In complex **3** the metal–metal distances are longer, the shortest of them being Mn(1)···Mn(2) of 5.642(3) Å observed in the dinuclear unit. These distances suggest that spin–spin magnetic interactions are unlikely to occur between the manganese ions of neighbouring chains or within the chain. However, the distortion of the manganese co-ordination octahedron in complexes **1** and **3** is large enough to result in a zero-field splitting of the manganese(II) ground state and to afford a small lowering of the magnetic moment at low temperature as previously observed for some manganese(II) complexes.[45]

The powder X-band EPR spectra of these two compounds exhibit only a temperature-independant and featureless single-line broad resonance with g values of 2.03 and 2.02 at room temperature for **1** and **3**, respectively. The broadness of these isotropic signals are in agreement with the results of the crystal structure determinations. The binuclear units are not isolated but bridged into infinite chains. In these polymeric structures intermolecular interactions, even if too small to be detected by magnetic susceptibility measurements, can constitute an effective pathway for spin–spin exchange interactions mediated by the lattice of chains.[46,47] Moreover, as observed by X-ray measurements there is a strong distortion from O_h symmetry so a zero-field splitting is expected but not observed. Axial distortion of the ligand field from octahedral have already been observed for some polymeric manganese(II) 4-methylpyridine compounds[48] without observation of zero-field splitting in the EPR spectra.

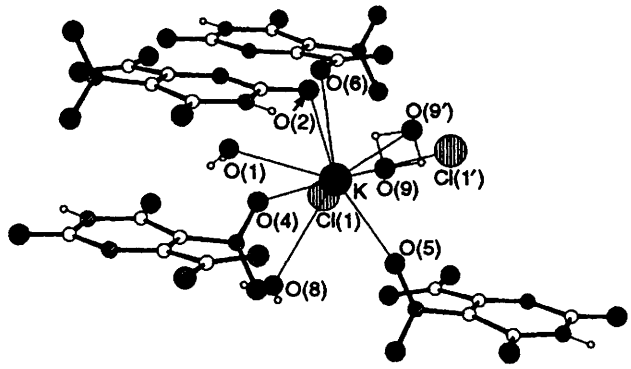

Fig. 6 Structure of the cation $[K_2(H_2O)]^{2+}$ and its surroundings in compound **3**

For complex **2** the effective magnetic moment per manganese(II) of 5.66 μ_B is lower than the spin-only value at 290 K and decreases over the entire temperature range explored, reaching 2.48 μ_B per Mn at 2 K indicating a net antiferromagnetic exchange interaction.

As already mentioned previously the structure consists of dinuclear units containing two high-spin manganese(II) ions bonded by one oxygen atom of the carboxylate group with a short Mn···Mn distance of 3.472(2) Å. Outwith this distance, the shortest Mn···Mn distances between two dinuclear units are in the order of 6.6 Å. Consequently, the interpretation of the variation of experimental magnetic susceptibility data with temperature was attempted by using the theoretical equation for an isotropic magnetic exchange interaction between two $S_1 = S_2 = \frac{5}{2}$ ions by employing the susceptibility equation $H = -2JS_1S_2$, the simplest spin Hamiltonian.[49,50]

The magnetic susceptibility equation used for this binuclear complex of manganese was that proposed by O'Connor[49] [equation (1)], where $x = J/kT$.

$$\chi = \frac{Ng^2\beta^2}{kT}\,\frac{2e^{2x} + 10e^{6x} + 28e^{12x} + 60e^{20x} + 110e^{30x}}{1 + 3e^{2x} + 5e^{6x} + 7e^{12x} + 9e^{20x} + 11e^{30x}} \quad (1)$$

The parameters obtained from the fit of the experimental values with this theoretical equation are $J = -1.3$ cm^{-1} and $g = 1.95$. A best fitting curve ($R = 6 \times 10^{-4}$) may be found for the same J and g values if a second term accounting for a paramagnetic impurity (5%) was added below 6 K. The values so obtained are quite similar to those obtained for dinuclear manganese(II) complexes with Robson-type ligands[50] ($J = -0.82$ cm^{-1} and $g = 1.94$). In the manganese chain species Mn_2(edta)·$9H_2O$ (edta = *N*,*N*,*N*',*N*'-ethylenediaminetetraacetate), values of $J = -0.50$ cm^{-1} and $g = 2.0$ are obtained; the weakness of the exchange observed in this case may be explained by the large distance between the two metal atoms (*ca.* 6 Å), the carboxylate group acting as an *anti-syn* bridge.[51]

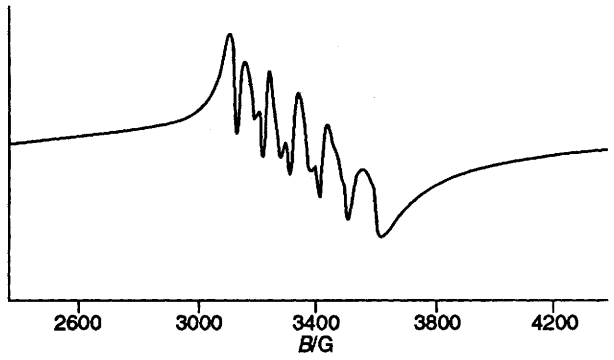

Fig. 7 Experimental EPR spectrum of complex **2** obtained as a frozen glass (water–ethylene glycol)

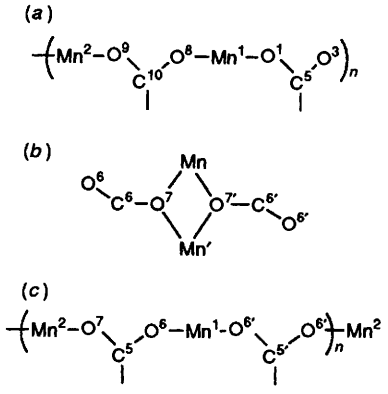

Fig. 8 Schematic representation of the carboxylate bridges between Mn^{II} ions in **1** (*a*), **2** (*b*) and **3** (*c*)

Complex **2** exhibits X-band powder EPR spectra characterized by a broad resonance centred near $g \approx 2$ which does not show appreciable temperature dependence. While frozen solution spectra obtained from water glasses also exhibit only a very broad isotropic resonance, the frozen solution spectra obtained from water–ethyleneglycol glasses at 100 K exhibit a central allowed hyperfine sextet (Fig. 7). The allowed hyperfine lines obey the condition $M = \frac{1}{2}$, $m \longleftrightarrow M = -\frac{1}{2}$, m; where M and m are the electronic and nuclear magnetic quantum numbers. Moreover we can observe the forbidden hyperfine lines corresponding to $M = \frac{1}{2}$, $m \longleftrightarrow M = -\frac{1}{2}$, $m - 1$ and $M = \frac{1}{2}$, $m - 1 \longleftrightarrow M = -\frac{1}{2}$, m. The forbidden doublet separation is defined to be the separation between the lines corresponding to $\frac{1}{2}$, $m \longleftrightarrow -\frac{1}{2}$, $m - 1$ and $\frac{1}{2}$, $m-1 \longleftrightarrow -\frac{1}{2}$, m.

This spectrum is typical for a Mn^{2+} ion and similar spectra have recently been observed by Misra[52] for Mn^{II} in SiO_2 xerogel samples and by Borras-Almenar *et al.*[53] from the X-band powder spectrum of Mn-doped $Zn_2(edta)\cdot 6H_2O$. By contrast, coupling two $S = \frac{5}{2}$ ions should give a system of 36 spin states which can be grouped into a six-spin manifold ($S = 0$, 1, 2, 3, 4 and 5). Nevertheless, the number of observed EPR transitions in the spectrum of a pair of Mn^{2+} ions may be much greater that the number observed for a monomeric complex.

The similarity of the fine-structure pattern of this complex with those described for electronically isolated manganese species indicates either that the dinuclear entity is not retained in dilute solution, or that the small antiferromagnetic interactions operating between the two manganese(II) ions of the binuclear unit do not modify appreciably the EPR spectra of these complexes.

The value of the hyperfine parameter A can be estimated from the average value of the separation between successive allowed hyperfine lines. The value of A is given by the expression proposed by Misra[52] [equation (2)] where B is the magnetic field.

$$B_m - B_{m-1} = \frac{A}{g\mu_B} - \frac{A^2}{8g^2\mu_B{}^2B_0}(2m - 1) \qquad (2)$$

Assuming $g = 2.00$, then we obtain $A = -0.27$ GHz. This value is in accord with those obtained by Narayana *et al.*,[54] Abragam and Bleaney[46] or more recently by Misra[52] for Mn^{2+} ions.

The zero-field splitting parameter (D) can be estimated by using the expression proposed by Misra[52] for the separation of a forbidden hyperfine doublet in the spectra of a polycrystalline sample. Taking into account the value of 20 G for the average forbidden doublet separation in our spectrum the value obtained is $D = \pm 2.93$ GHz. This low value of the zero-field splitting is indicative of a slightly distorted octahedral symmetry and does not reflect the steric constraints arising from the small bite angle N(1)–Mn–O(7) of 73.4(1)°. A complete study of the magnetic properties of this complex including single-crystal EPR studies is still in progress.

Conclusion

The reaction of Mn^{II} ion with H_3L^1, H_2L^2 and H_3L^3 in water at neutral pH has allowed the isolation of polynuclear metallic compounds. While complex **3** is rapidly obtained in the crystalline state from water–acetonitrile, compounds **1** and **2** were only obtained by slow evaporation of aqueous solutions. The UV absorption studies indicate the weak complexing properties of these ligands, at least in the case of H_3L^1 and H_3L^3. Then it seems likely that some modification in the crystallisation process could change the co-ordination and the structural arrangements of these manganese derivatives or could even lead to monomeric species as is generally reported for complexes of H_3L^1. However, it should be underlined that the major binding mode of the Mn^{II} ion in this class of ligand is *via* the N^1 and carboxylate sites in the solid state as well as in solution. Fig. 8 summarises the different modes of linking manganese atoms observed in the solid state. While X-ray diffraction studies show the polymeric nature of the complexes obtained, it should be noted that antiferromagnetic interaction between manganese(II) ions is only observed for the dinuclear complex obtained from H_2L^2.

Acknowledgements

We are grateful to the Université Paul Sabatier and to the European Community for financial support.

References

1 J. Leberman, A. Kornberg and E. S. Simms, *J. Biol. Chem.*, 1955, **215**, 403.
2 A. Lehninger, in *Principles of Biochemistry*, Worth Publishers Inc., New York, 1970, 661.
3 J. Victor, L. B. Greenberg and D. L. Sloan, *J. Biol. Chem.*, 1979, **254**, 2647.
4 E. R. Tucci, B. R. Doody and N. C. Li, *J. Phys. Chem.*, 1961, **65**, 1570.
5 M. Falk, *Pharmazie*, 1985, **40**, 377.
6 M. Sabat, D. Zlinska and B. Jezowska-Trzebiatowska, *Acta Crystallogr., Sect. B*, 1980, **36**, 1187.
7 I. Mutikainen and P. Lumme, *Acta Crystallogr., Sect. B*, 1980, **36**, 2233.
8 T. Solin, K. Matsumoto and K. Fuwa, *Bull. Chem. Soc. Jpn.*, 1981, **54**, 3731.
9 P. Arrizabalaga, P. Castan and F. Dahan, *Inorg. Chem.*, 1983, **22**, 2245.
10 I. Mutikainen, *Finn. Chem. Lett.*, 1985, 193.

11 M. Kubiac and B. Thomas, *Acta Crystallogr., Sect. C*, 1986, **42**, 1705.
12 I. Mutikainen, *Inorg. Chim. Acta*, 1987, **136**, 155.
13 I. Mutikainen, *Ann. Acad. Sci. Fen.*, 1988, **1**, 217 and refs. therein.
14 P. Castan, E. Colacio-Rodriguez, A. L. Beauchamp, S. Cros and S. Wimmer, *J. Inorg. Bio. Chem.*, 1990, **36**, 225.
15 D. Menitzafos, N. Katsaros and A. Terzis, *Acta Crystallogr., Sect. C*, 1987, **43**, 1905.
16 I. Bach, O. Kumberger and H. Schmidbaur, *Chem. Ber.*, 1990, **123**, 2267.
17 O. Kumberger, J. Riede and H. Schmidbaur, *Z. Naturforsch., Teil B*, 1993, **48**, 961.
18 Y. Kono, M. Takahashi and K. Asada, *Arch. Biochem. Biophys.*, 1976, **174**, 454; F. S. Archibald and I. Fridovich, *Arch. Biochem. Biophys.*, 1982, **214(2)**, 452.
19 F. J. Arnais Garcia, C. Capul, P. Castan, D. Deguenon, P. Derache and F. Nepveu, in *Metal ions in Biology and Medicine*, eds. P. Collery, L. A. Poirier, M. Manfait and J. C. Etienne, John Libbey Eurotext, Paris, 1990, p. 21; S. Rivomanana, M. Massol, P. Derache and F. Nepveu, in *Electron Spin Resonance (ESR), Applications in Organic and Bioorganic Materials*, ed. B. Catoire, Springer-Verlag, Berlin, 1992, p. 105.
20 M. Berkaoui, J. P. Souchard, M. Massol and F. Nepveu, *J. Chim. Phys.*, 1994, **91**, 1799.
21 C. Clerc-Bory and G. Mentzer, *Bull. Soc. Chim. Fr.*, 1958, 436.
22 P. Pascal, *Am. Chim. Phys. (Paris)*, 1910, **19**, 5.
23 G. M. Sheldrick, SHELXS 86, Program for the solution of crystal structures, University of Göttingen, 1986.
24 D. J. Watkin, J. R. Carruthers and P. W. Betteridge, CRYSTALS, Crystal user guide, Chemical Crystallography Laboratory, University of Oxford, 1985.
25 A. L. Spek, PLATON-90, Program for crystal structure determination, University of Utrech, 1990.
26 W. R. Busing, K. O. Martin and H. A. Levy, ORFFE-3, Report ORNL-TM-306, Oak Ridge National Laboratory, TN, 1971.
27 G. M. Sheldrick, SHELXTL PLUS, Nicolet Instrument Corporation, Madison, WI, 1987.
28 G. M. Sheldrick, SHELXL 93, University of Göttingen, 1993.
29 R. Hundt, KPLOT, University of Bonn, 1992.
30 *International Tables for X-Ray Crystallography*, Kynoch Press, Birmingham, 1974, vol. 4.
31 P. Castan, T. T. B. Ha, F. Nepveu and G. Bernardinelli, *Inorg. Chim. Acta*, 1994, **221**, 173.
32 E. R. Tucci and N. C. Li, *J. Inorg. Nucl. Chem.*, 1963, **25**, 17.
33 E. R. Tucci, C. H. Ke and N. C. Li, *J. Inorg. Nucl. Chem.*, 1967, **29**, 1657.
34 J. J. Fox, N. Yung and I. Wenpen, *Biochim. Biophys. Acta*, 1957, **23**, 295.
35 K. Inagaki and Y. Kidani, *Bioinorg. Chem.*, 1978, **9**, 157.
36 K. Nakanishi, N. Suzuki and F. Yamazaki, *Bull. Chem. Soc. Jpn.*, 1961, **34**, 53.
37 D. Lalart, G. Guillerez, G. Dodin and J.-E. Dubois, *J. Chem. Soc., Perkin Trans. 2*, 1981, 1057.
38 P. Arrizabalaga, P. Castan and J.-P. Laurent, *J. Inorg. Biochem.*, 1984, **20**, 215.
39 F. Takusagawa and A. Shimada, *Bull. Chem. Soc. Jpn.*, 1973, **46**, 2011.
40 J. H. Van Niekerk and F. R. L. Schoenig, *Acta Crystallogr.*, 1953, **6**, 227.
41 P. De Meester, S. R. Flecher and A. C. Skapski, *J. Chem. Soc., Dalton Trans.*, 1973, 2575.
42 R. J. Butcher, J. W. Overmann and E. Sinn, *J. Am. Chem. Soc.*, 1980, **102**, 3276.
43 A. M. Greenway, C. J. O'Connor, J. W. Overman and E. Sinn, *Inorg. Chem.*, 1981, **20**, 1506.
44 J. P. Costes, F. Dahan and J.-P. Laurent, *Inorg. Chem.*, 1985, **24**, 1118.
45 B. Mabad, P. Cassoux, J.-P. Tuchagues and D. N. Hendrickson, *Inorg. Chem.*, 1986, **35**, 1420.
46 A. Abragam and B. Bleaney, *Résonance Paramagnétique Electronique des Ions de Transition*, Presses Universitaires de France, Paris, 1971.
47 B. A. Goodman and J. B. Raynor, *Adv. Inorg. Chem. Radiochem.*, 1970, **13**, 205.
48 R. D. Dowsing, J. F. Gibson, M. Goodgame and P. J. Hayward, *J. Chem. Soc. A*, 1969, 187.
49 C. J. O'Connor, *Prog. Inorg. Chem.*, 1982, **29**, 203.
50 D. Luneau, J. M. Savariault, P. Cassoux and J.-P. Tuchagues, *J. Chem. Soc., Dalton Trans.*, 1988, 1225.
51 J. J. Borras-Almenar, R. Burriel, E. Coronado, D. Gatteschi, C. J. Gomez-Garcia and C. Zanchini, *Inorg. Chem.*, 1991, **30**, 947.
52 S. K. Misra, *Physica B*, 1994, 193.
53 J. J. Borras-Almenar, E. Coronado, D. Gatteschi and C. Zanchini, *Inorg. Chim. Acta*, 1993, **207**, 105.
54 N. Narayana, S. G. Sathyanarayan and G. Sivarama Sastry, *Ind. J. Pure Appl. Phys.*, 1976, **14**, 69.

Received 21*st April* 1995; *Paper* 5/02554K